



Published in final edited form as:

*Drug Discov Today Dis Models*. 2019 ; 29-30: 43–52. doi:10.1016/j.ddmod.2019.10.002.

## Diaphragm Muscle Adaptations in Health and Disease

Matthew J. Fogarty, Gary C. Sieck

Department of Physiology and Biomedical Engineering, Mayo Clinic, Rochester, MN, 55905, USA

### Abstract

Breathing is achieved without thought despite being controlled by a complex neural network. The diaphragm is the predominant muscle responsible for force/pressure generation during breathing, but it is also involved in other non-ventilatory expulsive behaviors. This review considers alterations in diaphragm muscle fiber types and the neural control of the diaphragm across our lifespan and in various disease conditions.

### Keywords

Spinal cord; neuromotor control; phrenic motor neuron; diaphragm motor unit

### Introduction:

The diaphragm muscle (DIAM) is unique to mammals, and separates the abdominal and thoracic cavities. The DIAM is the principal inspiratory pump muscle generating a negative intrathoracic pressure ( $P_{th}$ ) that drives air into the lungs during breathing. However, the DIAM also contributes to the generation of a positive intra-abdominal pressure ( $P_{ab}$ ), necessary for higher force expulsive behaviors (defecation, coughing and sneezing). The pressure difference across the thoracic/abdominal surfaces of the DIAM is the transdiaphragmatic pressures ( $P_{di}$ ) and can be measured as a surrogate for DIAM force generation (Figure 1). Repetitive activation of the DIAM during breathing involves a high duty cycle (time active versus inactive), but the  $P_{di}$  generated during even the most strenuous breathing efforts represent less than half of the maximum  $P_{di}$  ( $P_{di,max}$ ) that can be generated by the DIAM. In contrast, higher force expulsive behaviors are shorter in duration and non-repetitive. Thus, the design features for DIAM fibers activated during ventilatory versus expulsive behaviors are quite different. To accomplish repetitive lower force breathing efforts, it is necessary to recruit only fatigue resistant DIAM fibers. In contrast, for shorter duration higher force expulsive efforts, more fatigable DIAM fibers are recruited. The nervous system controls the recruitment of DIAM fibers through phrenic motor neurons

Address Correspondence to: Gary C. Sieck, PhD, Vernon F. and Earline D. Dale Professor, Department of Physiology & Biomedical Engineering, Mayo Clinic, 200 1<sup>st</sup> St SW, Rochester, MN 55905, Phone: (507) 284 6850, sieck.gary@mayo.edu.

**Publisher's Disclaimer:** This is a PDF file of an unedited manuscript that has been accepted for publication. As a service to our customers we are providing this early version of the manuscript. The manuscript will undergo copyediting, typesetting, and review of the resulting proof before it is published in its final form. Please note that during the production process errors may be discovered which could affect the content, and all legal disclaimers that apply to the journal pertain.

The Authors declare that there are no conflicts of interest, neither real nor perceived, with regards to the publication of this work.

(PhMNs) located in the cervical spinal cord. Collectively, a PhMN and the group of muscle fibers it innervated is termed a motor unit (Figure 2). The mechanical and fatigue properties of DIAM motor units are determined by the properties of the muscle fibers comprising the motor unit. Thus, there are slow- and fast-twitch motor units, and fatigue resistant and fatigable motor units. In this review, the effect of different disease conditions on DIAM motor units will be considered in the context of the impact on ventilatory versus expulsive behaviors of the DIAM.

### DIAM Fiber Type Classification:

Different isoforms of myosin heavy chain (MyHC) are expressed in the DIAM that determine both the contractile and fatigue properties of muscle fibers [1]. Some MyHC isoforms normally exist only during the embryonic (MyHC<sub>Emb</sub>) and neonatal (MyHC<sub>Neo</sub>) developmental periods of the DIAM [2, 3]. However, with muscle injury, the expression of MyHC<sub>Emb</sub> and MyHC<sub>Neo</sub> reappears, perhaps due to the fusion of satellite cells into injured fibers for repair [4–6]. In the normal adult DIAM, there are four MyHC isoforms that comprise four fiber types [1, 7–13]. A “slow” MyHC isoform (MyHC<sub>slow</sub>) is expressed in type I fibers, and there are three “fast” MyHC isoforms (MyHC<sub>2A</sub>, MyHC<sub>2X</sub>, MyHC<sub>2B</sub>) expressed in type IIa, and IIx and/or IIb fibers [8]. Type I fibers have a slower time to peak isometric force (i.e., slow twitch time), a slower maximum shortening velocity, generate lower specific force (force normalized per cross-sectional area), and are fatigue resistant during repetitive activation [1, 7, 14–16]. Type IIx and/or IIb DIAM fibers co-express MyHC<sub>2X</sub> and MyHC<sub>2B</sub> isoforms in varying proportions. These fast-twitch fibers have faster shortening velocities, generate greater specific force, and are more fatigable during repetitive stimulation. DIAM fiber type proportions can change under certain conditions, and this will influence the contractile and fatigue properties of DIAM [4–6]. However, caution should be taken in interpreting changes in fiber type proportions, since this may reflect dysregulation of MyHC isoform expression leading to co-expression of isoforms and ambiguous fiber type classification. Co-expression of MyHC isoforms in DIAM fibers has been noted in a variety of conditions [5, 17, 18].

### DIAM Fiber Force:

The sarcomere is the basic structural and functional unit of DIAM fibers. Actin filaments are anchored to Z-disks and project towards a midline (M-line). Each myosin filament is surrounded by six actin filaments, and Ca<sup>2+</sup> binding to troponin C on the actin filament regulates the attachment of myosin heads (MyHC) to the actin filament, forming cross-bridges that provide the molecular basis for contraction and force generation [19]. The force (F) generated by a single muscle fiber is estimated by the equation:

$$F = n \cdot f \cdot \alpha_{fs}$$

Where n is the MyHC concentration per half sarcomere, f is the force contributed by each cross-bridge and  $\alpha_{fs}$  is the proportion of MyHC heads forming tightly bound cross-bridges. As muscle fiber cross-sectional area increases (hypertrophy) or decreases (atrophy), n increases or decreases proportionately, such that the force per cross-sectional area (specific

force) of a fiber remains unchanged. However, there are many natural and pathological conditions where specific force of muscle fibers decreases (i.e., weakness). For example, during the perinatal period, the specific force of DIAM fibers is lower compared to adult fibers, due in part to a reduced  $n$  [8, 20]. Similarly, in old age, DIAM specific force is reduced compared to younger ages – sarcopenia [21–26]. Furthermore, with chronic obstructive pulmonary disease (COPD) [27–30], cachexia [31, 32], corticosteroid treatment [33–37], hypothyroidism [38–40], and malnutrition [41–50], specific force of the DIAM is reduced, indicating that  $n$  can be affected, most likely via proteolysis rather than reduced synthesis of MyHC [4].

The force generated by an individual cross-bridge ( $f$ ) is mainly determined by MyHC isoform, being lower in fibers expressing MyHC<sub>slow</sub> compared to fast MyHC isoforms [8, 51]. The  $f$  for a specific MyHC isoform may be affected in some conditions; however, this can only be determined using a single fiber preparation where force and  $n$  are both measured. For example, following denervation, DIAM specific force decreases due to a decrease in both  $n$  and  $f$  [52, 53]. Similarly, with COPD in humans, DIAM fiber specific force decreases due to both a decrease  $n$  and  $f$  [30].

### Ca<sup>2+</sup> Sensitivity of DIAM Force:

At optimal sarcomere length (i.e., greatest extent of overlap of myosin heads with actin binding sites), the primary determinant of  $\alpha_{fs}$  is Ca<sup>2+</sup> regulation of myosin binding to actin (force-Ca<sup>2+</sup> relationship). Type I DIAM fibers display greater Ca<sup>2+</sup> sensitivity compared to all type II fibers (leftward shift in the force-Ca<sup>2+</sup> relationship) [51]. This most likely reflects the expression of a “slow” isoform of troponin C with only two Ca<sup>2+</sup> binding sites. In COPD patients, Ca<sup>2+</sup> sensitivity of DIAM fiber force decreases, possibly reflecting the co-expression of MyHC and troponin C isoforms [30].

### DIAM Force-Length Relationship:

At sub-optimal length, some myosin heads cannot bind to actin; thus, even during maximum Ca<sup>2+</sup> activation,  $\alpha_{fs}$  is reduced and less force is generated (force-length relationship). In COPD, the DIAM flattens due to retention of air in the lungs, and at least initially, this will affect the DIAM force-length relationship contributing to a reduction in force. However, with time, there is length adaptation in the COPD DIAM, with a reduction in the number of sarcomeres in series [27, 54]. Thus, an optimal length for force is re-established.

### DIAM Fiber Energetic Balance:

Cross-bridge cycling requires ATP hydrolysis and depends on external load (Figure 3). Cross-bridge cycling and ATP hydrolysis rates vary across DIAM fiber types, being greater in type II fibers comprising MyHC<sub>2A</sub>, MyHC<sub>2X</sub>, MyHC<sub>2B</sub> isoforms compared to type I fibers comprising the MyHC<sub>slow</sub> isoform. The consumption of ATP for any MyHC isoform is described by the equation:

$$\text{ATP Consumption} = n \cdot b \cdot \alpha_{fs} \cdot g_{app}$$

Where  $b$  is the number of half sarcomeres in series and  $g_{app}$  is the apparent rate constant for cross bridge detachment.

Velocity of shortening and  $g_{app}$  are dependent on external loading; thus, ATP consumption changes with external load and the velocity of shortening, reaching a maximum at the peak power output of a muscle fiber (Figure 3) [9, 55, 56]. In order to accommodate the sizeable range of ATP consumption demands across different DIAM fiber types, there is also considerable range in the reserve capacity for ATP production via mitochondrial oxidative phosphorylation. Due to the higher mitochondrial volume densities of type I and IIa fibers DIAM fibers and thus their higher oxidative capacities, the reserve capacity for ATP production in these fibers is quite high compared to type IIx and/or IIb fibers [57, 58]. Type IIx and/or IIb fibers depend more on glycolytic pathways for ATP production, with a much lower functional reserve capacity. Accordingly, it is likely that the higher rates of ATP consumption, lower mitochondrial volume density and oxidative capacity, and thus, lower reserve capacity for ATP production in type IIx and/or IIb fibers underlies their greater fatigue susceptibility [7, 13]. Mitochondrial production of ATP via oxidative phosphorylation in type I and IIa DIAM fibers is much higher, which when combined with their slower cross-bridge cycling rates and ATP consumption rates [57, 58] contributes to their increased endurance (fatigue resistance). In this respect, it is noteworthy that with aging, the residual force maintained by the DIAM after repetitive activation is unaffected [23], indicating the energetic resilience of type I and IIa fibers. Unfortunately, very few if any studies have systematically explored the impact of diseases (e.g., COPD, diabetes) or conditions (e.g., aging, malnutrition) on energetic balance of DIAM fibers.

### Training Effects:

Throughout life, skeletal muscle is constantly remodeled, adjusting to vagaries in activity, load, or innervation. Thus, within limits, muscle fibers can adapt to environmental conditions, changing their structure and function to suit new natural or imposed scenarios. This is commonly observed in sports, where athletes train to achieve desired muscle adaptations that optimize performance needs. For example, mitochondrial biogenesis can improve muscle endurance via an increase in mitochondrial volume density and oxidative capacity. An increase in the external load on muscle fibers leads to an increase in fiber cross-sectional area thereby adding sarcomeres in parallel, increasing MyHC concentration per half sarcomere ( $n$  in the equation above) and increasing muscle strength. There is no reason to doubt that the DIAM responds in a similar fashion to improve endurance and/or strength. However, it should be considered that the DIAM is a highly active muscle with a breathing duty cycle (time active versus inactive) of ~40%. Thus, those DIAM fibers that are active with breathing are essentially endurance trained and may not respond to a further increase in activity compared to limb muscle fibers with a much lower duty cycle. In contrast, it is very likely that DIAM fibers will respond to resistance/strength training, but this does not target breathing efforts.

The importance of skeletal muscle remodeling extends far beyond exercise physiology to many clinical conditions and diseases. The strength and endurance of various muscles changes throughout life, even without exercise (e.g., early postnatal development and old

age). Chronic diseases, including diabetes, heart disease, cancer cachexia, etc. result in muscle wasting, weakening and diminished endurance. Additionally, neuromuscular or muscular diseases such as muscular dystrophy and other congenital muscular disorders, amyotrophic lateral sclerosis (ALS), and spinal cord injury may impair DIAM performance. A variety of therapeutic conditions including corticosteroid treatment and mechanical ventilation may also impact DIAM function. Of considerable interest is the fact that these effects are predominantly reflected by an atrophy (reduced cross sectional area) of type IIx and/or IIb fibers, resulting in weakness (reduced maximum force) with little initial impact on endurance during breathing [14, 23, 26, 57, 59–63]. Consistent with these results, endurance training has not been shown to be effective. Just as the mode of exercise varies for training marathon runners versus body builders, there is not a single therapeutic approach to mitigate the impact of disease on the DIAM.

### Motor Units in the DIAM:

The final executor of neural control of the DIAM is the PhMN, which evokes contraction of the muscle fibers it innervates (i.e., DIAM motor unit activation; Figure 2). PhMNs are located in the cervical spinal cord (C<sub>3</sub>-C<sub>6</sub> depending on species). In the mouse and rat, there are ~200–240 PhMNs on each side [64–66], providing a total of ~400–480 DIAM motor units that affect motor control across a range of motor behaviors. In the adult rat, PhMNs vary ~8-fold in size with somal surface areas ranging from ~1,000 to 8,000  $\mu\text{m}^2$  [64–66] and this size variability plays an important role in motor control. During embryonic and early postnatal development, the size of PhMNs is more homogenous, with a subsequent growth of larger PhMNs into adulthood [65, 67, 68]. This increase in PhMN size corresponds to the emergence of type IIx and/or IIb fibers in the DIAM [65]. In older rats, there is an ~25% age-related loss of larger PhMNs that may underlie sarcopenia of old age [26, 64]. Recently, we reported that PhMN size varies with DIAM paralysis induced by spinal cord hemisection (shift to smaller size) compared to tetrodotoxin (TTX) blockade of phrenic nerve action potential propagation (shift toward larger PhMNs) [69]. Unfortunately, no studies have explored whether changes in PhMN morphology are induced by chronic disease.

The size of PhMNs is matched to the mechanical and fatigue properties of the DIAM fibers they innervate. Importantly, all DIAM fibers comprising an individual DIAM motor unit express the same contractile proteins and share similar biochemical properties (i.e., they are the same muscle fiber type; Figure 2) [1, 7, 11, 70–74]. Slow-twitch, type S DIAM motor units comprise type I fibers that generate less force but are fatigue resistant [13, 73]. It is likely that type S motor units comprise smaller PhMNs, although this has not been directly established. Fast-twitch, fatigue resistant (type FR) DIAM motor units comprise type IIa fibers that also generate lower specific force compared to other fast motor units but greater than type I fibers [8, 20, 52, 75]. More fatiguable fast-twitch motor units comprise type IIx and/or IIb DIAM fibers that co-express MyHC<sub>2X</sub> and/or MyHC<sub>2B</sub> isoforms in varying proportions accounting for intermediate (type FInt) to greater fatigability (type FF). The type IIx/IIb DIAM fibers comprising FInt and FF DIAM fibers have larger cross-sectional areas [47, 50, 65, 76] and generate greater specific forces compared to type I and IIa fibers [8, 51]. Thus, their contribution to total DIAM force is proportionately greater.

DIAM motor unit innervation ratio (i.e., number of muscle fibers innervated by a PhMN) is an important contributor to unit force generation. In rats, there are ~400 to 480 PhMNs [64], that innervate ~48,000 DIAM fibers, with an average innervation ratio ~100 to 120 fibers [77]. Of note, in the cat DIAM, we determined the innervation ratio of different motor unit types using a glycogen depletion method and found an innervation ratio of ~120 fibers per motor unit with no difference across motor unit types [12, 78, 79].

With advanced age, the total number of PhMNs decreases primarily impacting larger PhMNs that innervate type FInt and FF DIAM motor units [64]. This age-related loss of PhMNs results in initial denervation of type IIX and/or IIB DIAM fibers. Importantly, we previously found that DIAM denervation is associated with atrophy of type IIX and/or IIB fibers and a decrease in specific force [52, 76], similar to sarcopenia. Interestingly, neither denervation or age affects the cross-sectional areas of type I and IIA DIAM fibers. With time, the age-related loss of PhMNs is accompanied by axonal sprouting of surviving PhMNs, reinnervation of type IIX and/or IIB fibers and expansion of motor unit innervation ratio.

During embryonic and early postnatal development, DIAM fibers can be innervated by more than one PhMN (polyneuronal innervation) [14, 80]. The disappearance of polyneuronal innervation of DIAM fibers by the second postnatal week in rats coincides with the emergence of type IIX and/or IIB fibers [14, 20, 75, 80, 81], suggesting that some trophic relationship between larger PhMNs and type IIX and/or IIB DIAM fibers may exist. This is supported by studies showing that unilateral denervation of the DIAM in the first postnatal week in rats results in stunted growth of type IIX and/or IIB fibers on the affected side. It is important to note however that ventilation is not affected by unilateral DIAM denervation [82].

A loss of PhMNs may also occur in other disease conditions, most notably amyotrophic lateral sclerosis (ALS). Importantly ALS also appears to affect larger motor neurons [83–86], and this may explain the initial maintenance of ventilation in ALS patients. However, ALS patients are at increased risk for airway infections and pneumonias [87–89], perhaps reflecting their inability to effectively clear their airways. Other neural degenerative diseases may also differentially affect larger PhMNs, but no systematic analysis has been performed.

### Neural Control of $P_{di}$ in Different Motor Behaviors:

Due to the high duty cycle requirements to sustain ventilation, the inspiratory pump function of the DIAM must involve generation of non-fatiguing  $P_{di}$ . Although a positive  $P_{ab}$  is generated with each breath, expiration is typically passive driven by elastic recoil of the lungs and chest wall. Active recruitment of the DIAM and other abdominal wall muscles to generate higher force  $P_{di}$  is more infrequent (i.e., a lower duty cycle). These higher force expulsive behaviors often require near-maximal activation of the DIAM. Accordingly, the morphological and functional design of the DIAM involves two groups of motor units: one a lower force but fatigue resistant set of motor units (type S and FR comprising type I and IIA fibers) that are efficiently designed to generate adequate  $P_{di}$  to sustain breathing, and a second set of higher force but fatigable motor units (type FInt and FF comprising type IIX

and/or IIB fibers) that are optimally designed for short duration bursts of near-maximal  $P_{di}$  [14].

Neuromotor control of the DIAM to generate  $P_{di}$  during different motor behaviors is accomplished by recruitment and rate coding of motor units. The recruitment order of DIAM motor units is determined by the intrinsic size-dependent electrophysiological properties of PhMNs [16, 85, 90–92] described by the following equation:

$$dV_m/dt = I_{syn}/C_m$$

Where  $dV_m/dt$  is the change in membrane potential,  $I_{syn}$  is the synaptic current and  $C_m$  is membrane capacitance. Thus, for a given  $I_{syn}$ , smaller PhMNs with less surface area and lower  $C_m$  have a greater  $dV_m/dt$  compared to larger PhMNs with greater  $C_m$ . Smaller PhMNs are more excitable reaching a threshold for action potential generation sooner. It is widely assumed that smaller PhMNs innervate fatigue resistant type S and FR DIAM motor units, whereas larger PhMNs innervate type FInt and FF motor units, and that an orderly recruitment of motor units occurs across the range of forces required for different motor behaviors (Figure 2). This recruitment order is maintained even with increasing neural drive ( $I_{syn}$ ), but there is a decrease in delay before recruiting motor units and an increase in discharge rate [93].

Based on the assumption of an orderly size-dependent recruitment of PhMNs, we developed a model for DIAM motor unit recruitment (Figure 2) [7, 12, 16, 79, 94, 95]. Our initial model for the cat DIAM, was based on direct measurements of motor unit force and estimates of the contribution of each motor unit type compared to  $P_{di_{max}}$  generated by bilateral phrenic nerve stimulation [7, 16, 60, 79, 96, 97]. Subsequently, in rodent DIAM, the force contribution of different motor unit types was estimated based on measurements of  $Ca^{2+}$  activated specific force generated by different types of single permeabilized DIAM fibers [8, 51], their mean cross-sectional areas [47, 50, 65], the relative fiber type proportion [1, 7, 73] and the assumption of similar innervation ratios across motor unit types [12, 78, 79]. In each of these models, ventilatory behaviors (i.e., eupnea, hypoxia/hypercapnia, sighs and airway occlusion) were accomplished by the recruitment of only type S and FR motor units [12, 16, 79, 98, 99]. It was determined that during eupnea and hypoxia/hypercapnia the DIAM generates <15% of  $P_{di_{max}}$  [1, 7, 16, 26, 59]. Sighs are spontaneous deep inspirations that have a  $P_{di}$  amplitude >2-fold tidal breaths. During airway occlusion, as occurs during obstructive sleep apnea,  $P_{di}$  approaches ~40–50%  $P_{di_{max}}$ , and this maximum ventilatory-related effort is largely accomplished by maximal recruitment of type S and FR motor units with some minimal recruitment of FInt motor units [23]. However, to perform higher force, expulsive behaviors (i.e., coughing, sneezing, defecation), the recruitment of additional type FInt and FF motor units is required [12, 16, 79, 98, 99].

There are only a few studies that have assessed the increase in  $P_{di}$  during exercise as ventilatory or abdominal core requirements increase. During exercise intensities inducing maximum minute ventilation ( $V_{E_{max}}$ ), tidal volume can increase by ~5-fold from eupneic

levels, presumably requiring increased  $P_{di}$  generation. In previous studies, we examined maximum voluntary ventilation (MVV) under isocapnic conditions in human subjects, which ranged from ~180 to 230 L/min in healthy young subjects [100, 101]. However, MVV cannot be sustained and rapidly declines within ~2 min to a maximum sustainable ventilatory capacity (MSVC) of ~60% MVV (Figure 4). In addition, changes in DIAM EMG spectral content occur indicating DIAM fatigue. Thus, it appears that some more fatigable DIAM motor units can be recruited during more extreme ventilatory efforts. The  $V_{E_{max}}$  in normal subjects does not exceed MSVC. However, there is some evidence that under conditions of intense exercise in highly trained individuals DIAM fatigue occurs [102], indicating that the recruitment of more fatigable DIAM motor units may limit exercise performance in some individuals. During non-ventilatory body core exercises (e.g., weight lifting, sit-ups), the DIAM is more active, and a level of ~50%  $P_{di_{max}}$  has been reported [103], but this  $P_{di}$  would not necessarily require recruitment of more fatigable DIAM motor units.

As the superior wall of the abdominal cavity, the DIAM is indispensable in the generation of positive  $P_{ab}$  for a variety of motor behaviors. Indeed, many of the non-ventilatory behaviors of the DIAM are associated with the generation of extremely high forces and thus necessitate the extensive recruitment of PhMNs and DIAM motor units [14]. The highest  $P_{ab}$  are generated during straining behaviors (e.g., defecation, vomiting, and parturition) that consist of very high levels of DIAM activation with co-contraction of external intercostal and abdominal muscles, while simultaneously closing of the glottis by coordinated activation of the laryngeal lateral cricoarytenoid and transverse arytenoid muscles [104]. Synchronous co-contraction of the abdominal muscles and DIAM against a closed airway prevents their relative shortening [105, 106], ensuring that the optimal lengths of these muscles are maintained throughout the duration of activation. Preserved optimal lengths during voluntarily expulsive Valsalva maneuvers in humans explain why the  $P_{di}$  generated is so high (e.g.,  $P_{di}$  up to 220 cmH<sub>2</sub>O) [107–109]. Coughing and sneezing are expulsive airway clearance behaviors that require coordinated co-activation of the DIAM and abdominal muscles. During forceful coughing and sneezing the  $P_{di}$  generated can approach  $P_{di_{max}}$ . Even when the abdominal muscles are paralyzed in quadriplegic patients, DIAM activation is still preserved during coughing efforts [110]. It is important to recognize that while expulsive straining behaviors require the generation of very high DIAM forces/ $P_{di}$ , these pressures do not need to be sustained for long-periods of time. Thus, DIAM fatigue is not a factor unless these behaviors are repeated, e.g., parturition, chronic coughing [14, 85]. Parturition is associated with very forceful co-activation of the DIAM and abdominal muscles, which is prolonged and repeated. Coordinated contractions of the DIAM and abdominal muscles can generate intra-uterine pressures of ~170–300 cmH<sub>2</sub>O [111–113]. Thus, it is not surprising that DIAM fatigue may occur during labor [114]. In addition, DIAM injury may occur during high-force expulsive efforts associated with parturition [115–122] as well as coughing [123–127], vomiting [128] or defecation. In fact, non-traumatic DIAM herniation is commonly reported in association straining behaviors [129]. Conversely, patients who have severe DIAM weakness, report difficulties with coughing and defecation [130].

## References

1. Sieck GC, Fournier M, and Enad JG, Fiber type composition of muscle units in the cat diaphragm. *Neurosci Letters*, 1989 97(1–2): p. 29–34.
2. Watchko JF, et al., Contractile properties of the rat external abdominal oblique and diaphragm muscles during development. *J Appl Physiol*, 1992 72(4): p. 1432–1436. [PubMed: 1592735]
3. Watchko JF and Sieck GC, Respiratory muscle fatigue resistance relates to myosin phenotype and SDH activity during development. *J Appl Physiol*, 1993 75: p. 1341–1347. [PubMed: 8226549]
4. Argadine HM, et al., The effect of denervation on protein synthesis and degradation in adult rat diaphragm muscle. *J Appl Physiol*, 2009 107(2): p. 438–44. [PubMed: 19520837]
5. Schiaffino S, et al., Embryonic and neonatal myosin heavy chain in denervated and paralyzed rat skeletal muscle. *Dev Biol*, 1988 127(1): p. 1–11. [PubMed: 3282936]
6. Carraro U, et al., Chronic denervation of rat hemidiaphragm: Maintenance of fiber heterogeneity with associated increasing uniformity of myosin isoforms. *J Cell Biol*, 1985 100(1): p. 161–174. [PubMed: 3965469]
7. Fournier M and Sieck GC, Mechanical properties of muscle units in the cat diaphragm. *J Neurophysiol*, 1988 59(3): p. 1055–1066. [PubMed: 3367195]
8. Geiger PC, et al., Maximum specific force depends on myosin heavy chain content in rat diaphragm muscle fibers. *J Appl Physiol*, 2000 89(2): p. 695–703. [PubMed: 10926656]
9. Han YS, et al., ATP consumption rate per cross bridge depends on myosin heavy chain isoform. *J Appl Physiol*, 2003 94(6): p. 2188–96. [PubMed: 12588786]
10. Johnson BD and Sieck GC, Differential susceptibility of diaphragm muscle fibers to neuromuscular transmission failure. *J Appl Physiol*, 1993 75(1): p. 341–348. [PubMed: 8397179]
11. Johnson BD, et al., Contractile properties of the developing diaphragm correlate with myosin heavy chain phenotype. *J Appl Physiol*, 1994 77: p. 481–487. [PubMed: 7961272]
12. Sieck GC, Neural control of the inspiratory pump. *NIPS*, 1991 6: p. 260–264.
13. Sieck GC, et al., Myosin phenotype and SDH enzyme variability among motor unit fibers. *J Appl Physiol*, 1996 80(6): p. 2179–2189. [PubMed: 8806928]
14. Fogarty MJ and Sieck GC, Evolution and Functional Differentiation of the Diaphragm Muscle of Mammals. *Compr Physiol*, 2019 9(2): p. 715–766. [PubMed: 30873594]
15. Krnjevic K and Miledi R, Motor units in the rat diaphragm. *J Physiol*, 1958 140: p. 427–439. [PubMed: 13514716]
16. Sieck GC and Fournier M, Diaphragm motor unit recruitment during ventilatory and nonventilatory behaviors. *J Appl Physiol*, 1989 66(6): p. 2539–2545. [PubMed: 2745316]
17. Gosker HR, et al., Skeletal muscle fibre-type shifting and metabolic profile in patients with chronic obstructive pulmonary disease. *Eur Respir J*, 2002 19(4): p. 617–25. [PubMed: 11998989]
18. Rowan SL, et al., Denervation causes fiber atrophy and myosin heavy chain co-expression in senescent skeletal muscle. *PLoS One*, 2012 7(1): p. e29082. [PubMed: 22235261]
19. Plowman S and Smith D, Exercise physiology for health, fitness, and performance. 1997, Boston, Mass: Allyn & Bacon.
20. Geiger PC, et al., Mechanisms underlying increased force generation by rat diaphragm muscle fibers during development. *J Appl Physiol*, 2001 90: p. 380–388. [PubMed: 11133931]
21. Elliott JE, et al., Diaphragm muscle sarcopenia in Fischer 344 and Brown Norway rats. *Experimental physiology*, 2016 101(7): p. 883–94. [PubMed: 27126607]
22. Fogarty MJ, et al., Diaphragm neuromuscular transmission failure in aged rats. *J Neurophysiol*, 2019 122(1): p. 93–104. [PubMed: 31042426]
23. Fogarty MJ, Mantilla CB, and Sieck GC, Impact of sarcopenia on diaphragm muscle fatigue. *Exp Physiol*, 2019 104(7): p. 1090–1099. [PubMed: 30924589]
24. Gosselin LE, Johnson BD, and Sieck GC, Age-related changes in diaphragm muscle contractile properties and myosin heavy chain isoforms. *Am J Respir Crit Care Med*, 1994 150: p. 174–178. [PubMed: 8025746]
25. Greising SM, et al., Diaphragm muscle sarcopenia in aging mice. *Exp Gerontol*, 2013 48(9): p. 881–887. [PubMed: 23792145]

26. Khurram OU, et al., Impact of aging on diaphragm muscle function in male and female Fischer 344 rats. *Physiol Rep*, 2018 6(13): p. e13786. [PubMed: 29981218]
27. Levine S, et al., Human diaphragm remodeling associated with chronic obstructive pulmonary disease: clinical implications. *Am J Respir Crit Care Med*, 2003 168(6): p. 706–13. [PubMed: 12857719]
28. Mantilla CB and Sieck GC, Neuromotor Control in Chronic Obstructive Pulmonary Disease. *J Appl Physiol*, 2013 114: p. 1246–52. [PubMed: 23329816]
29. Ottenheijm CA, et al., Titin and diaphragm dysfunction in chronic obstructive pulmonary disease. *Am J Respir Crit Care Med*, 2006 173(5): p. 527–34. [PubMed: 16339921]
30. Ottenheijm CA, et al., Diaphragm dysfunction in chronic obstructive pulmonary disease. *Am J Respir Crit Care Med*, 2005 172(2): p. 200–5. [PubMed: 15849324]
31. Roberts BM, et al., Diaphragm and ventilatory dysfunction during cancer cachexia. *FASEB J*, 2013 27(7): p. 2600–10. [PubMed: 23515443]
32. Roberts BM, et al., Cancer cachexia decreases specific force and accelerates fatigue in limb muscle. *Biochem Biophys Res Commun*, 2013 435(3): p. 488–92. [PubMed: 23673294]
33. Dekhuijzen PNR, Corticosteroid treatment and nutritional deprivation cause a different pattern of atrophy in rat diaphragm. *J Appl Physiol*, 1995 78: p. 629–637. [PubMed: 7759433]
34. Koerts-de Lang E, et al., Different effects of corticosteroid-induced muscle wasting compared with undernutrition on rat diaphragm energy metabolism. *Eur J Appl Physiol*, 2000 82(5–6): p. 493–8. [PubMed: 10985606]
35. Lewis MI, Monn SA, and Sieck GC, Effect of corticosteroids on diaphragm fatigue, SDH activity, and muscle fiber size. *J Appl Physiol*, 1992 72(1): p. 293–301. [PubMed: 1537729]
36. Sassoon CS, et al., Interactive effects of corticosteroid and mechanical ventilation on diaphragm muscle function. *Muscle & nerve*, 2011 43(1): p. 103–11. [PubMed: 21171101]
37. van Balkom RHH, et al., Corticosteroid effects on isotonic contractile properties of rat diaphragm muscle. *J Appl Physiol*, 1997 83: p. 1062–1067. [PubMed: 9338411]
38. Geiger PC, et al., Effects of hypothyroidism on maximum specific force in rat diaphragm muscle fibers. *J Appl Physiol*, 2002 92(4): p. 1506–1514. [PubMed: 11896017]
39. Herb RA, et al., Alterations in phenotypic and contractile properties of the rat diaphragm: influence of hypothyroidism. *J Appl Physiol*, 1996 80(6): p. 2163–70. [PubMed: 8806926]
40. Sieck GC, et al., Hypothyroidism alters diaphragm muscle development. *J Appl Physiol*, 1996 81: p. 1965–1972. [PubMed: 8941517]
41. Brozanski BS, et al., Effect of undernutrition on contractile and fatigue properties of rat diaphragm during development. *J Appl Physiol*, 1993 74(5): p. 2121–6. [PubMed: 8335538]
42. Koerts-De Lang E, et al., Contractile properties and histochemical characteristics of the rat diaphragm after prolonged triamcinolone treatment and nutritional deprivation. *Journal of muscle research and cell motility*, 1998 19(5): p. 549–55. [PubMed: 9682141]
43. Lewis MI, et al., Effect of severe short-term malnutrition on diaphragm muscle signal transduction pathways influencing protein turnover. *J Appl Physiol*, 2006 100(6): p. 1799–806. [PubMed: 16484360]
44. Lewis MI, Feinberg AT, and Fournier M, IGF-I and/or growth hormone preserve diaphragm fiber size with moderate malnutrition. *J. Appl. Physiol*, 1998 85: p. 189–197. [PubMed: 9655774]
45. Lewis MI, et al., Interactive effects of denervation and malnutrition on diaphragm structure and function. *J Appl Physiol*, 1996 81: p. 2165–2172. [PubMed: 8941542]
46. Lewis MI, et al., Interactive effects of emphysema and malnutrition on diaphragm structure and function. *J Appl Physiol*, 1994 77(2): p. 947–55. [PubMed: 8002552]
47. Lewis MI and Sieck GC, Effect of acute nutritional deprivation on diaphragm structure and function. *J Appl Physiol*, 1990 68: p. 1938–1944. [PubMed: 2163377]
48. Lewis MI and Sieck GC, Effect of acute nutritional deprivation on diaphragm structure and function in adolescent rats. *J Appl Physiol*, 1992 73(3): p. 974–978. [PubMed: 1400065]
49. Prakash YS, Fournier M, and Sieck GC, Effects of prenatal undernutrition on developing rat diaphragm. *J Appl Physiol*, 1993 75: p. 1044–1052. [PubMed: 8226510]

50. Sieck GC, Lewis MI, and Blanco CE, Effects of undernutrition on diaphragm fiber size, SDH activity, and fatigue resistance. *J Appl Physiol*, 1989 66: p. 2196–2205. [PubMed: 2745285]
51. Geiger PC, Cody MJ, and Sieck GC, Force-calcium relationship depends on myosin heavy chain and troponin isoforms in rat diaphragm muscle fibers. *J Appl Physiol*, 1999 87(5): p. 1894–1900. [PubMed: 10562634]
52. Geiger PC, et al., Denervation-induced changes in myosin heavy chain expression in the rat diaphragm muscle. *J Appl Physiol*, 2003 95(2): p. 611–619. [PubMed: 12704093]
53. Han YS, et al., Effects of denervation on mechanical and energetic properties of single fibers in rat diaphragm muscle. *Biophysical J*, 1999 76(1): p. A34.
54. Moore AJ, et al., Passive properties of the diaphragm in COPD. *Journal of applied physiology*, 2006 101(5): p. 1400–5. [PubMed: 16840573]
55. Han YS, et al., Reserve capacity of ATP consumption during isometric contraction in human skeletal muscle fibers. *J Appl Physiol*, 2001 90: p. 657–664. [PubMed: 11160066]
56. Sieck GC, et al., Cross-bridge cycling kinetics, actomyosin ATPase activity and myosin heavy chain isoforms in skeletal and smooth respiratory muscles. *Comp Biochem Physiol*, 1998 119(3): p. 435–450.
57. Rowley KL, Mantilla CB, and Sieck GC, Respiratory muscle plasticity. *Respir Physiol Neurobiol*, 2005 147(2–3): p. 235–51. [PubMed: 15871925]
58. Sieck GC, et al., Changes in actomyosin ATP consumption rate in rat diaphragm muscle fibers during postnatal development. *J. Appl. Physiol*, 2003 94: p. 1896–1902. [PubMed: 12562672]
59. Khurram OU, et al., Diaphragm muscle function following midcervical contusion injury in rats. *J Appl Physiol* (1985), 2019 126(1): p. 221–230. [PubMed: 30236045]
60. Sieck GC, Diaphragm motor units and their response to altered use. *Sem Respir Med*, 1991 12: p. 258–269.
61. Fogarty MJ, Mantilla CB, and Sieck GC, Breathing: Motor Control of Diaphragm Muscle. *Physiology* (Bethesda), 2018 33(2): p. 113–126. [PubMed: 29412056]
62. Gransee HM, Mantilla CB, and Sieck GC, Respiratory Muscle Plasticity. *Compr Physiol*, 2012 2(2): p. 1441–1462. [PubMed: 23798306]
63. Mantilla CB and Sieck GC, Neuromuscular adaptations to respiratory muscle inactivity. *Respir Physiol Neurobiol*, 2009 169(2): p. 133–40. [PubMed: 19744580]
64. Fogarty MJ, et al., Phrenic Motor Neuron Loss in Aged Rats. *J Neurophysiol*, 2018.
65. Prakash YS, et al., Phrenic motoneuron morphology during rapid diaphragm muscle growth. *J Appl Physiol*, 2000 89(2): p. 563–72. [PubMed: 10926639]
66. Rana S, Sieck GC, and Mantilla CB, Diaphragm electromyographic activity following unilateral midcervical contusion injury in rats. *J Neurophysiol*, 2017 117(2): p. 545–555. [PubMed: 27832610]
67. Fogarty MJ, et al., Genetic deficiency of GABA differentially regulates respiratory and non-respiratory motor neuron development. *PLoS ONE*, 2013 8(2): p. e56257. [PubMed: 23457538]
68. Fogarty MJ, et al., Genetic absence of the vesicular inhibitory amino acid transporter differentially regulates respiratory and locomotor motor neuron development. *Brain Struct Funct*, 2015 220(1): p. 525–40. [PubMed: 24276495]
69. Mantilla CB, et al., Phrenic motoneuron structural plasticity across models of diaphragm muscle paralysis. *J Comp Neurol*, 2018 526(18): p. 2973–2983. [PubMed: 30411341]
70. Hamm TM, et al., Association between biochemical and physiological properties in single motor units. *Muscle Nerve*, 1988 11(3): p. 245–254. [PubMed: 3352659]
71. Nemeth PM, et al., Application of cross-sectional single-fiber microchemistry to the study of motor-unit fatigability, in *Motor Control*, Gantchev GN, Dimitrov B, and Gatev P, Editors. 1986, Plenum: New York.
72. Nemeth PM, et al., Uniformity of metabolic enzymes within individual motor units. *J Neurosci*, 1986 6(3): p. 892–898. [PubMed: 3958798]
73. Enad JG, Fournier M, and Sieck GC, Oxidative capacity and capillary density of diaphragm motor units. *J Appl Physiol*, 1989 67((2)): p. 620–627. [PubMed: 2529236]

74. Sieck GC, et al., Muscle fiber type distribution and architecture of the cat diaphragm. *J Appl Physiol*, 1983 55(5): p. 1386–1392. [PubMed: 6643176]
75. Geiger PC, et al., Mechanisms underlying myosin heavy chain expression during development of the rat diaphragm muscle. *J Appl Physiol*, 2006 101(6): p. 1546–55. [PubMed: 16873604]
76. Miyata H, et al., Myoneural interactions affect diaphragm muscle adaptations to inactivity. *J Appl Physiol*, 1995 79: p. 1640–1649. [PubMed: 8594024]
77. Fournier M and Sieck GC, Somatotopy in the segmental innervation of the cat diaphragm. *J Appl Physiol*, 1988 64: p. 291–298. [PubMed: 3356649]
78. Fournier M and Sieck GC, Topographical projections of phrenic motoneurons and motor unit territories in the cat diaphragm, in *Respiratory Muscles and Their Neuromotor Control*, Sieck GC, Gandevia SC, and Cameron WE, Editors. 1987, Alan R. Liss, Inc.: New York p. 215–226.
79. Sieck GC, Organization and recruitment of diaphragm motor units, in *The Thorax*, Roussos C, Editor. 1995, Marcel Dekker: New York, NY p. 783–820.
80. Mantilla CB, et al., Functional Development of Respiratory Muscles, in *Fetal and Neonatal Physiology*, Polin R, et al., Editors. 2016, Elsevier: Philadelphia.
81. Mantilla CB, et al., Developmental effects on myonuclear domain size of rat diaphragm fibers. *J Appl Physiol*, 2008 104(3): p. 787–94. [PubMed: 18187618]
82. Gill LC, Mantilla CB, and Sieck GC, Impact of unilateral denervation on transdiaphragmatic pressure. *Respir Physiol Neurobiol*, 2015 210: p. 14–21. [PubMed: 25641347]
83. Fogarty MJ, Driven to decay: Excitability and synaptic abnormalities in amyotrophic lateral sclerosis. *Brain Res Bull*, 2018 140: p. 318–333. [PubMed: 29870780]
84. Fogarty MJ, The bigger they are the harder they fall: size-dependent vulnerability of motor neurons in amyotrophic lateral sclerosis. *J Physiol*, 2018 596(13): p. 2471–2472. [PubMed: 29719046]
85. Fogarty MJ, et al., Size-dependent vulnerability of lumbar motor neuron dendritic degeneration in SOD1G93A mice. *Anat Rec (Hoboken)*, 2019 In Press.
86. Dukkipati SS, Garrett TL, and Elbasiouny SM, The vulnerability of spinal motoneurons and soma size plasticity in a mouse model of amyotrophic lateral sclerosis. *J Physiol*, 2018 596(9): p. 1723–1745. [PubMed: 29502344]
87. Gil J, et al., Causes of death amongst French patients with amyotrophic lateral sclerosis: a prospective study. *Eur J Neurol*, 2008 15(11): p. 1245–51. [PubMed: 18973614]
88. Leone M, Chandra V, and Schoenberg BS, Motor neuron disease in the United States, 1971 and 1973–1978: patterns of mortality and associated conditions at the time of death. *Neurology*, 1987 37(8): p. 1339–43. [PubMed: 3614653]
89. Spataro R, et al., Causes and place of death in Italian patients with amyotrophic lateral sclerosis. *Acta Neurol Scand*, 2010 122(3): p. 217–23. [PubMed: 20078446]
90. Cullheim S, et al., Membrane area and dendritic structure in type-identified triceps surae alpha motoneurons. *J Comp Neurol*, 1987 255(1): p. 68–81. [PubMed: 3819010]
91. Butler JE, McKenzie DK, and Gandevia SC, Discharge properties and recruitment of human diaphragmatic motor units during voluntary inspiratory tasks. *J Physiol*, 1999 518 (Pt 3): p. 907–20. [PubMed: 10420024]
92. Kernell D, *The motoneurone and its muscle fibres*. 2006, New York: Oxford University Press Inc.
93. Seven YB, et al., Non-stationarity and power spectral shifts in EMG activity reflect motor unit recruitment in rat diaphragm muscle. *Respir Physiol Neurobiol*, 2013 185(2): p. 400–9. [PubMed: 22986086]
94. Seven YB, Mantilla CB, and Sieck GC, Recruitment of Rat Diaphragm Motor Units Across Motor Behaviors with Different Levels of Diaphragm Activation. *J Appl Physiol*, 2014 117(11): p. 1308–16. [PubMed: 25257864]
95. Sieck GC, Recruitment of diaphragm motor units during ventilatory and non-ventilatory behaviors, in *Motor Control VII. Proceedings of the VIIth International Symposium on Motor Control*, Borovets, Bulgaria, Stuart DG, et al., Editors. 1996, Motor Control Press: Tucson, AZ p. 39–42.
96. Sieck GC, Diaphragm muscle: Structural and functional organization. *Clin Chest Med*, 1988 9(2): p. 195–210. [PubMed: 3292123]

97. Sieck GC and Fournier M, Contractile and fatigue properties of diaphragm motor units, in *Respiratory Muscles and Their Neuromotor Control*, Sieck GC, Gandevia SC, and Cameron WE, Editors. 1987, Alan R. Liss, Inc: New York p. 227–237.
98. Sieck GC, Recruitment and frequency coding of diaphragm motor units during ventilatory and non-ventilatory behaviors, in *Respiratory Control*, Swanson GD, Grodins FS, and Hughson RL, Editors. 1989, Plenum Press: New York p. 441–450.
99. Sieck GC, Conceptual model of ventilatory muscle recruitment and diaphragmatic fatigue, in *Modeling and Parameter Estimation in Respiratory Control*, Khoo MCK, Editor. 1990, Plenum Press: New York p. 113–123.
100. Belman MJ and Sieck GC, The ventilatory muscles: Fatigue, endurance and training. *Chest*, 1982 82: p. 761–766. [PubMed: 6754275]
101. Sieck GC, Mazar A, and Belman MJ, Changes in diaphragmatic EMG spectra during hyperpneic loads. *Respir Physiol*, 1985 61: p. 137–152. [PubMed: 4048666]
102. Coast JR, et al., Maximal inspiratory pressure following maximal exercise in trained and untrained subjects. *Med Sci Sports Exerc*, 1990 22(6): p. 811–815. [PubMed: 2287259]
103. Strongoli LM, Gomez CL, and Coast JR, The effect of core exercises on transdiaphragmatic pressure. *J Sports Sci Med*, 2010 9(2): p. 270–4. [PubMed: 24149695]
104. Iscoe S, Control of abdominal muscles. *Prog Neurobiol*, 1998 56(4): p. 433–506. [PubMed: 9775401]
105. Ait-Haddou R, Binding P, and Herzog W, Theoretical considerations on cocontraction of sets of agonistic and antagonistic muscles. *J Biomech*, 2000 33(9): p. 1105–11. [PubMed: 10854883]
106. Herzog W and Ait-Haddou R, Considerations on muscle contraction. *J Electromyogr Kinesiol*, 2002 12(6): p. 425–33. [PubMed: 12435539]
107. Cobb WS, et al., Normal intraabdominal pressure in healthy adults. *J Surg Res*, 2005 129(2): p. 231–5. [PubMed: 16140336]
108. Hackett DA and Chow CM, The Valsalva maneuver: its effect on intra-abdominal pressure and safety issues during resistance exercise. *J Strength Cond Res*, 2013 27(8): p. 2338–45. [PubMed: 23222073]
109. Shaw JM, et al., Intra-abdominal pressures during activity in women using an intra-vaginal pressure transducer. *J Sports Sci*, 2014 32(12): p. 1176–85. [PubMed: 24575741]
110. Estenne M and Gorini M, Action of the diaphragm during cough in tetraplegic subjects. *J Appl Physiol* (1985), 1992 72(3): p. 1074–80. [PubMed: 1568963]
111. Buhimschi CS, et al., Use of McRoberts' position during delivery and increase in pushing efficiency. *Lancet*, 2001 358(9280): p. 470–1. [PubMed: 11513914]
112. Pierce SL, et al., In vivo measurement of intrauterine pressure by telemetry: a new approach for studying parturition in mouse models. *Physiol Genomics*, 2010 42(2): p. 310–6. [PubMed: 20460604]
113. Rada CC, et al., Intrauterine telemetry to measure mouse contractile pressure in vivo. *J Vis Exp*, 2015(98): p. e52541. [PubMed: 25867820]
114. Nava S, et al., Evidence of acute diaphragmatic fatigue in a “natural” condition. The diaphragm during labor. *Am Rev Respir Dis*, 1992 146(5 Pt 1): p. 1226–30. [PubMed: 1443875]
115. Boufettal R, et al., [Spontaneous diaphragm rupture during delivery. Case report]. *J Gynecol Obstet Biol Reprod (Paris)*, 2008 37(1): p. 93–6. [PubMed: 18077103]
116. Hamaji M, et al., Spontaneous diaphragm rupture associated with vaginal delivery. *Gen Thorac Cardiovasc Surg*, 2013 61(8): p. 473–5. [PubMed: 22930128]
117. Hamoudi D, et al., Diaphragmatic rupture during labor. *Int J Obstet Anesth*, 2004 13(4): p. 284–6. [PubMed: 15477063]
118. Hill R and Heller MB, Diaphragmatic rupture complicating labor. *Ann Emerg Med*, 1996 27(4): p. 522–4. [PubMed: 8604875]
119. Ross DB and Stiles GE, Spontaneous rupture of the diaphragm in labour: a case report. *Can J Surg*, 1989 32(3): p. 212–3. [PubMed: 2713776]

120. Rubin S, et al., Diaphragmatic rupture during labour, two years after an intra-oesophageal rupture of a bronchogenic cyst treated by an omental wrapping. *Interact Cardiovasc Thorac Surg*, 2009 9(2): p. 374–6. [PubMed: 19423509]
121. Servais EL, et al., Ruptured diaphragmatic eventration: a rare cause of acute postpartum dyspnea. *Ann Thorac Surg*, 2012 93(6): p. e143–4. [PubMed: 22632531]
122. Zimmermann T, [An unusual trauma in labor: diaphragmatic rupture]. *Zentralbl Gynakol*, 1999 121(2): p. 92–4. [PubMed: 10096176]
123. Chaar CI, Attanasio P, and Detterbeck F, Disruption of the costal margin with transdiaphragmatic abdominal herniation induced by coughing. *Am Surg*, 2008 74(4): p. 350–3. [PubMed: 18453304]
124. Daniel R, Naidu B, and Khalil-Marzouk J, Cough-induced rib fracture and diaphragmatic rupture resulting in simultaneous abdominal visceral herniation into the left hemithorax and subcutaneously. *Eur J Cardiothorac Surg*, 2008 34(4): p. 914–5. [PubMed: 18715797]
125. George L, Rehman SU, and Khan FA, Diaphragmatic rupture: A complication of violent cough. *Chest*, 2000 117(4): p. 1200–1. [PubMed: 10767262]
126. Kallay N, et al., Massive left diaphragmatic separation and rupture due to coughing during an asthma exacerbation. *South Med J*, 2000 93(7): p. 729–31. [PubMed: 10923968]
127. Rogers FB, Leavitt BJ, and Jensen PE, Traumatic transdiaphragmatic intercostal hernia secondary to coughing: case report and review of the literature. *J Trauma*, 1996 41(5): p. 902–3. [PubMed: 8913225]
128. Lee HY, et al., Spontaneous diaphragmatic rupture after vomiting: rapid diagnosis on multiplanar reformatted multidetector CT. *J Thorac Imaging*, 2006 21(1): p. 54–6. [PubMed: 16538159]
129. Edwin F, et al., eComment: Spontaneous or effort diaphragmatic rupture. *Interact Cardiovasc Thorac Surg*, 2009 9(2): p. 376. [PubMed: 19628553]
130. Perry SF, et al., The evolutionary origin of the mammalian diaphragm. *Respir Physiol Neurobiol*, 2010 171(1): p. 1–16. [PubMed: 20080210]

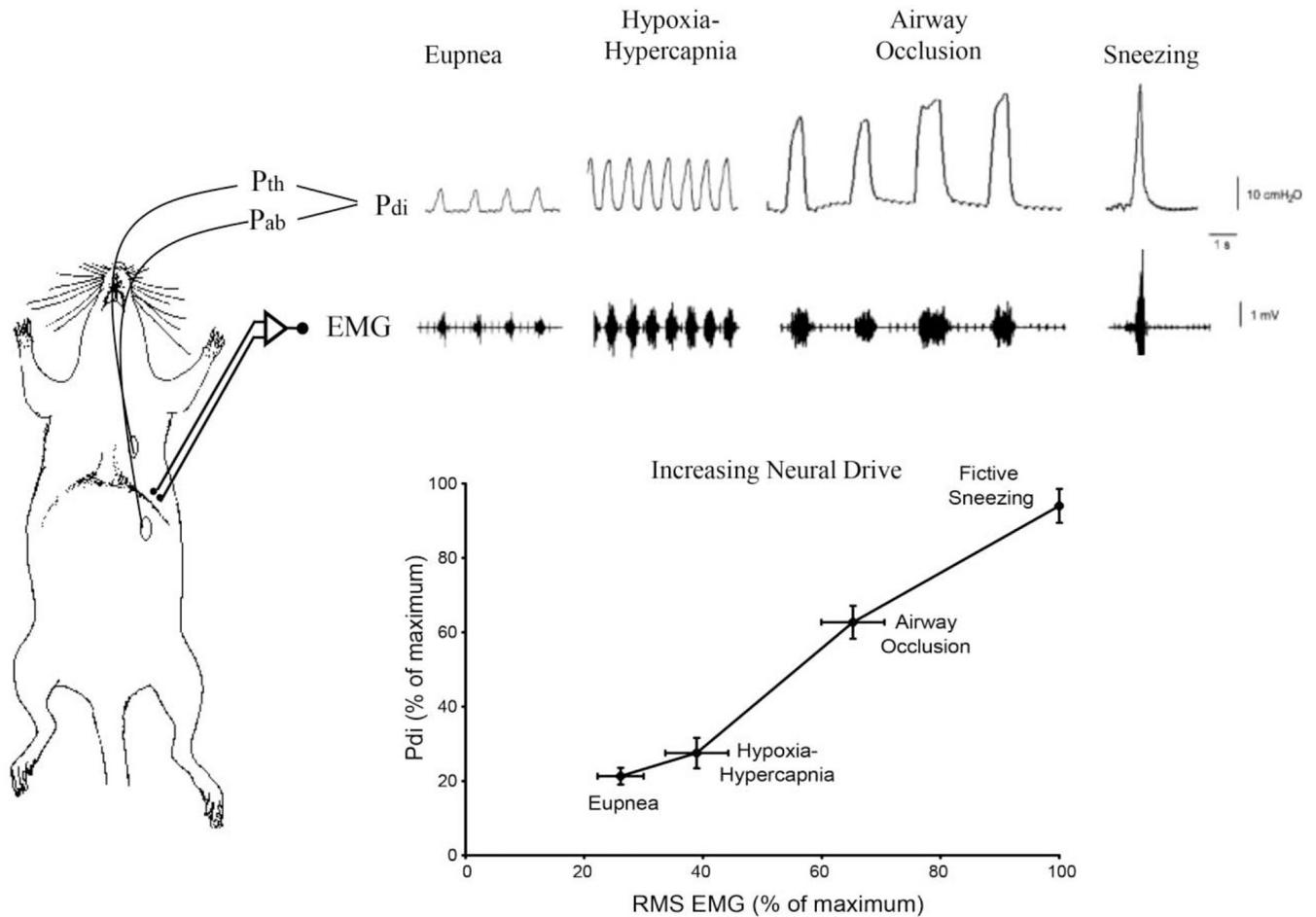


**Figure 1:**

Anatomical schematic illustrating oesophageal and gastric placement of the solid-state pressure catheters measuring the intra-thoracic ( $P_{th}$ ) and intra-abdominal ( $P_{ab}$ ) pressures in rodents. Negative  $P_{th}$  during DIAM contraction causes inspiratory airflow. Caudal motion of DIAM during contraction also produces a positive  $P_{ab}$ . The resulting transdiaphragmatic pressure ( $P_{di} = P_{ab} - P_{th}$ ) reflects the magnitude of DIAM force generation. Traces show representative  $P_{di}$  and raw electromyographic (EMG) measurements obtained in a rat across different ventilatory (eupnea, hypoxia/hypercapnia and occlusion) and non-ventilatory behaviors ('sneezing' induced by airway irritation with capsaicin). The graph depicts the relationship between DIAM EMG activity (maximum RMS EMG amplitude) and  $P_{di}$  measurements across different behaviors in adult rats. All values are normalized to  $P_{di\max}$ , achieved with bilateral phrenic nerve stimulation. Both RMS EMG and  $P_{di}$  increased progressively from eupnea to hypoxia-hypercapnia to airway occlusion to sneezing. The  $P_{di}$  and RMS EMG generated during occlusion and fictive sneezing was significantly greater than that generated during eupnea or hypoxia-hypercapnia.

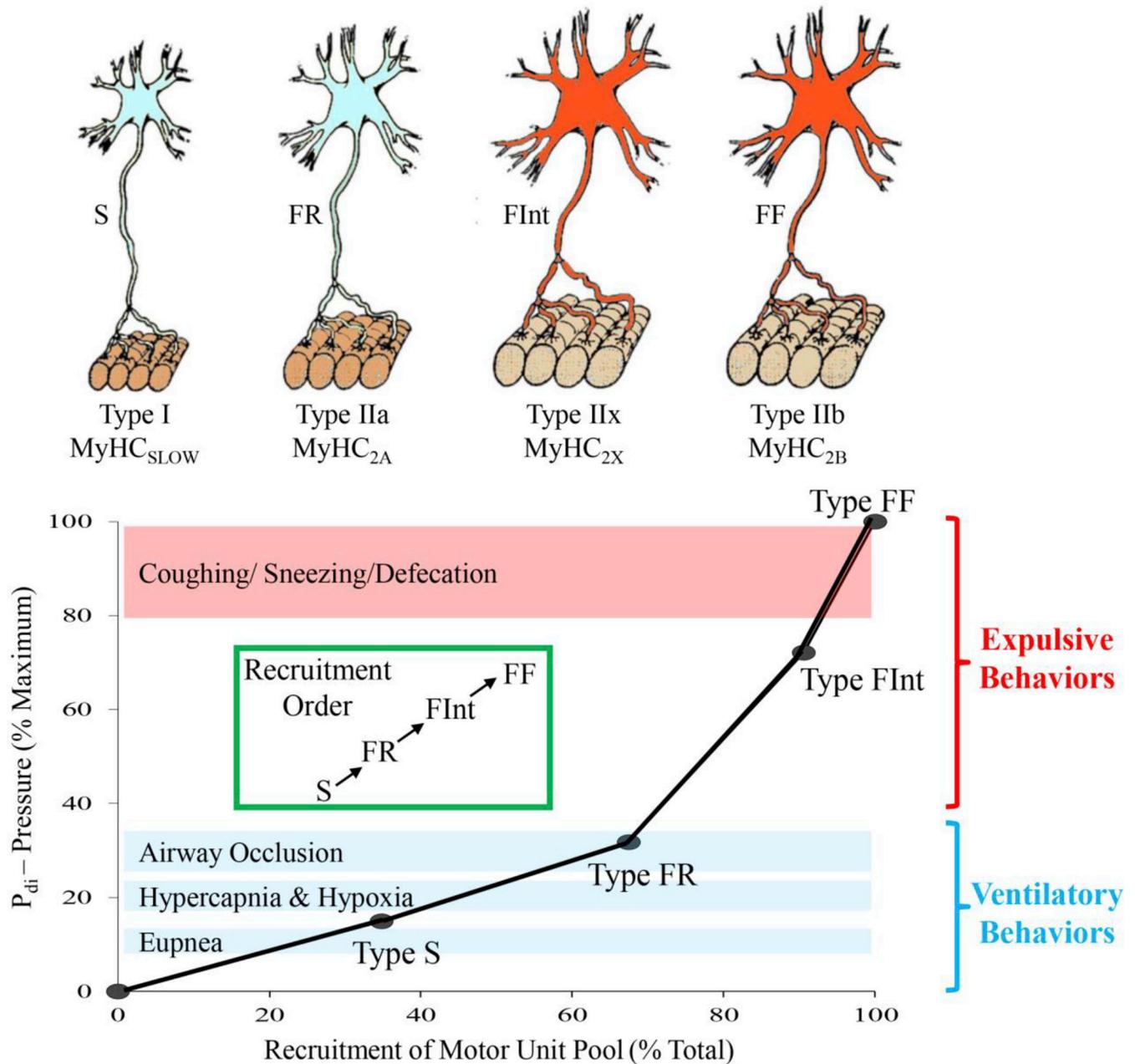


**Figure 2:**

Different DIAM motor unit types are distinguished by their intrinsic, mechanical, and fatigue properties, and are classified as type S, FR, FInt, and FF. Within an individual motor unit, all constituent muscle fibers exhibit homogeneous myosin heavy chain (MyHC) expression. In the DIAM of most species, type I and IIa muscle fibers have smaller cross-sectional areas than those of type IIx and/or IIb fibers. Differences in specific force between different fiber types is related to the different MyHC content per half sarcomere and the differing unitary forces produced by different MyHC isoforms, such that forces produced by type I fibers are less than forces produced by type IIa fibers that are less than forces produced by IIx and/or IIb fibers. Recruitment of DIAM motor units is in an orderly fashion, necessary to

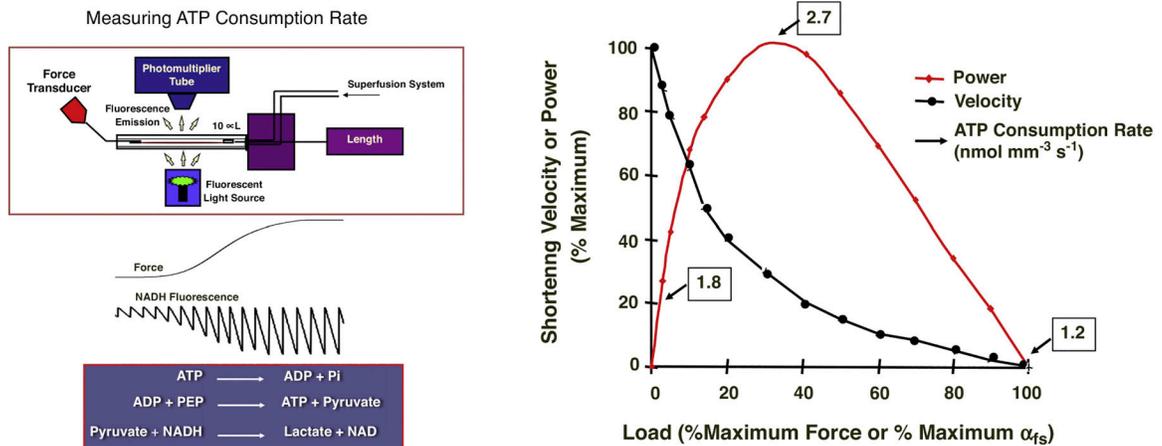
accomplish a range of motor behaviors. Ventilation (eupnea, hypoxia/hypercapnia and breathing against occlusion) is accomplished by recruitment type S and FR motor units, whereas higher-force airway clearance behaviors and straining/expulsive manoeuvres require recruitment of more fatigable type FIInt and FF motor units. Adapted from elements within [14].

Author Manuscript

Author Manuscript

Author Manuscript

Author Manuscript



*Drug Discovery Today: Disease Models*

**Figure 3:**

Simultaneous measurement of ATP consumption rate and force production in single permeabilized DIAM fibers is achieved by use of a perfusion cuvette. In the presence of activating or relaxing solutions, DIAM fiber isometric force is measured by a force transducer. ATPase activity was measured at 15°C by using a fluorescence-coupled enzyme assay, which involves the following reactions: i) ATP is hydrolyzed by the actomyosin ATPase to ADP and inorganic phosphate (Pi); ii) ATP is regenerated from ADP and PEP by PK; and iii) the resulting pyruvate is converted to lactate by LDH, which results in stoichiometric conversion of fluorescent NADH to nonfluorescent  $\text{NAD}^+$ . For each 1 mole of ADP produced by actomyosin ATPase, 1 mole of NADH is converted to  $\text{NAD}^+$ . Thus, the amount of ADP production by is determined by measuring the decrease in NADH fluorescence after stopping the flow in the cuvette. In single DIAM fibers, peak ATP consumption rates ( $2.7 \text{ nmol mm}^{-3} \text{ s}^{-1}$ ) occur at peak power output. The shortening velocity is reduced with loading.

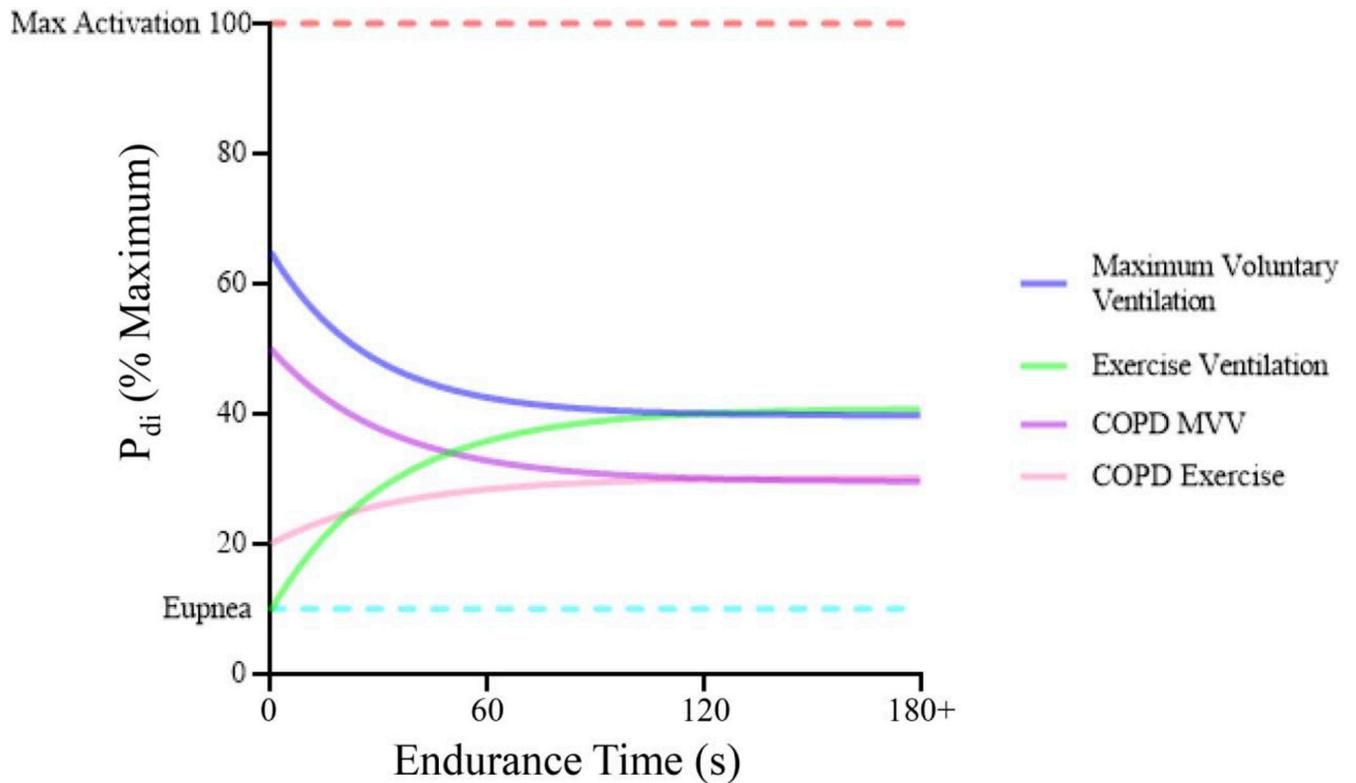


**Figure 4:**

Maximum voluntary ventilation (MVV) efforts approach ~60–70% of the maximum activation ( $P_{di}$ ) of the DIAM. These efforts cannot be maintained and fatigue occurs at a level of ~60% of this effort, or ~40% of the maximum activation. By contrast, exercise increases activation until all fatigue resistant (type S and type FR) motor units are recruited. This level of activation, ~40% of maximum  $P_{di}$  can be maintained indefinitely. In scenarios where there are altered chest mechanics (eg. COPD), both MVV and exercise ventilation are reduced. Sadly, systematic assessments of  $P_{di}$  during disease conditions or exercise are lacking, particularly in relation to maximum  $P_{di}$ .